

Active Probe Control of a Metrological Atomic Force Microscopy

J. C. Shen¹, N. Dorozhovets², T. Hausotte², E. Manske², W. Y. Jywe¹ and C. H. Liu³

¹Department of Automation Engineering, National Formosa University, Huwei, Yunlin, 632, Taiwan (e-mail: jcshen@nfu.edu.tw).

²Faculty of Mechanical Engineering, Institute of Process Measurement and Sensor Technology, Ilmenau University of Technology, Ilmenau, Thuringia, Germany.

³Institute of Electro-Optical and Materials Science, National Formosa University, Huwei, Yunlin, 632, Taiwan.

Abstract: This article considers the force control of an active probe for Atomic Force Microscopy (AFM). Firstly, the structure of this active probe is described. For designing the force controller, the model of this active probe was identified. Based on the measured frequency response, two notch filters were used to remove the resonant peak in open-loop frequency response. Then, a PI controller was designed to regulate the force of the probe. This controller was then implemented in a Digital Signal Processor (DSP). Experimental results were given to compare the actual performance of this controller with the conventional PI controller. It is shown that the controller with notch filters reduces the control error considerably and enables faster scan speed at weaker tip-sample interaction forces.

Keywords: Atomic force microscope, Force control, PI controller, Notch filters.

1. INTRODUCTION

Atomic Force Microscope (AFM) is an important instrument in the field of nanotechnology. It is used in investigation and manipulation on the nanometre scale (Binnig et al., 1986). In an AFM, a probe tip supported on a micro-mechanical cantilever is used to scan the surface of the sample, a displacement unit is used to move the sample under the tip (or the tip over the sample), a detecting system for sensing the position and deflection of the tip, a feedback system to control the deflection of the cantilever and finally a computer system to control the displacement unit, measure data and convert the data into an image (Sarid, 1994). Most of the AFM use the piezoelectric actuators to provide the scanning motion with a relatively small scanning window of about $100\mu\text{m} \times 100\mu\text{m}$ (Merry et al., 2009). Today's technological progress in electronics, the semiconductor industry, biotechnology, precision technology and many others requires metrological accurate object measurement with nanometre precision over large ranges (mm ranges). Such measurements are only possible if the measuring and positioning systems have good metrological characteristics and are traceable to national and international normal standards (Jaeger, 2010). In order to meet these requirements, a metrological large scan ranges AFM has been developed at the Institute of Process Measurement and Sensor Technology of the Ilmenau University of Technology (Dorozhovets et al., 2006a, b, 2008). This AFM includes an active scanning probe and a nano-positioning and nano-measuring (NPM) machine which has a positioning and measuring range of $25\text{mm} \times 25\text{mm} \times 5\text{mm}$ and a resolution of 0.1nm.

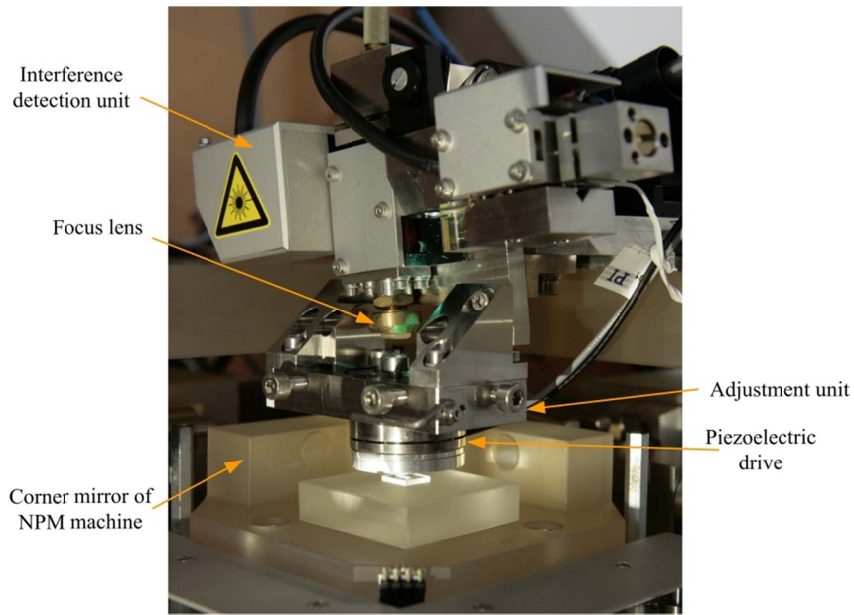
In this paper, the force control of the active probe of the metrological large ranges AFM that developed at the Institute

of Process Measurement and Sensor Technology of the Ilmenau University of Technology is considered. In general, probing of the sample surface can be performed in contact mode, non-contact mode or intermittent-contact (tapping) mode. In this paper, we only consider contact mode. In this mode, the tip and sample are in contact at all times and the force between the tip and the sample should keep at a desired constant value in a closed-loop operation. Generally, in commercial realizations a proportional integral (PI) controller is used to operate this loop and the bandwidth of the loop is tuned far below the first resonance frequency (Schitter et al. 2004, Zou et al., 2004, Abramovitch et al., 2009). Thus the scan speed is limited. Recently, some researchers utilized more sophisticated controllers (for example, H^∞ theory based controller) to improve the control performance (Schitter et al. 2004, Zou et al., 2004, Merry et al., 2009). However, the order of this kind of controller is high. This may cause some problems when implementing the controller.

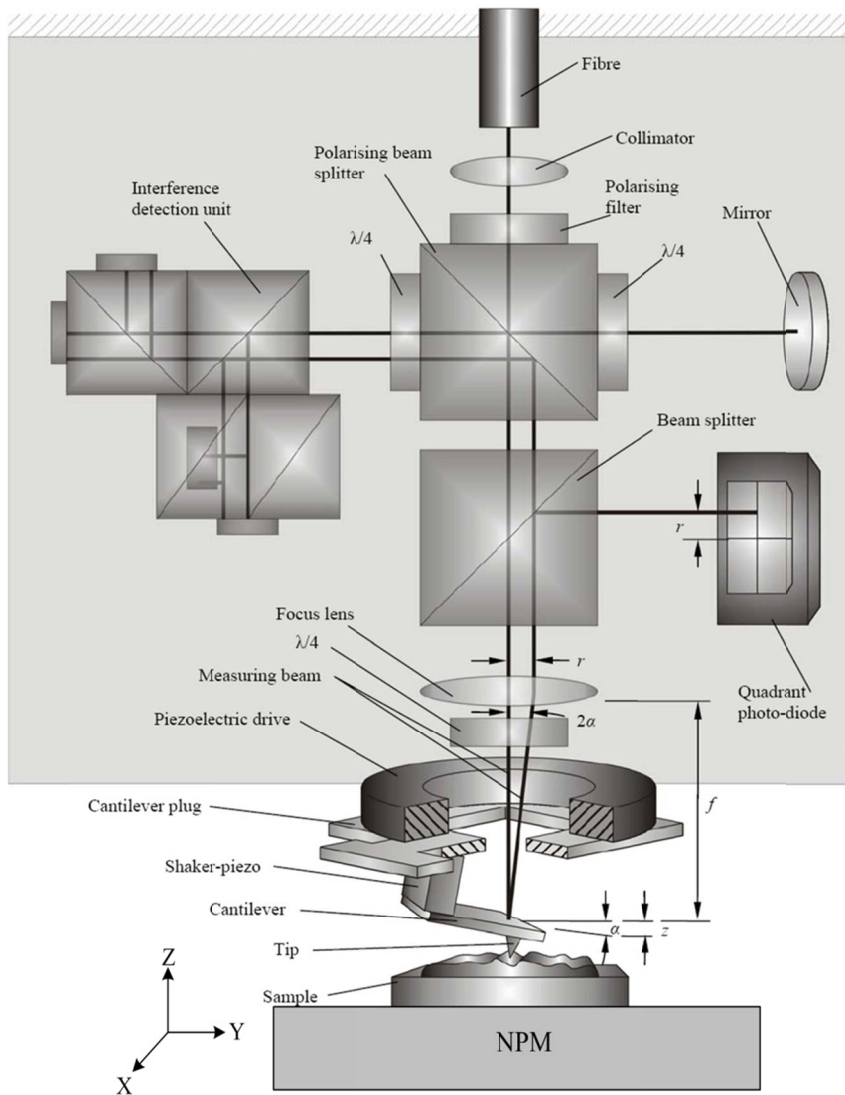
In this study, notch filters are used to improve the performance of the control loop. Firstly, the metrological large range AFM is described in Section 2. For designing the controller, the frequency response of the active probe is measured and a mathematical model is obtained in Section 3. Section 4 describes the design of the controller. In Section 5, scan results obtained by a PI controlled AFM are compared with the results obtained by the AFM that controlled by the proposed controller. Conclusions are given in Section 6.

2. THE METROLOGICAL AFM

The photograph and schematic representation of the metrological AFM are shown in Fig.1. This AFM includes an active scanning probe and a NPM machine. The sample for scanning is placed on the moveable corner mirror of the NPM



(a) The photograph of the metrological AFM.



(b) The schematic representation of the metrological AFM.

Fig. 1. The photograph and the schematic representation of the metrological AFM.

machine which has a positioning and measuring range of 25mm × 25mm × 5mm with a resolution of 0.1 nm and a positioning uncertainty of 10 nm.

In the active probe, only one measuring laser beam is used. The laser light source is coupled with the AFM probe head by fiber optic cable. The polarizing light is collimated by a lens. In the homodyne interference detection system, a fraction of the laser power that serves as a reference beam is divided by a polarizing beam splitter and is injected to a reference mirror. The measuring beam then focused on the cantilever end by using a focus lens because the width of the cantilever is smaller than the diameter of the collimated laser beam used; however, interferometer function is not affected. The reflected light then split after passing the lens again. One part of the measuring beam is directed onto a quadrant photodiode, which determines the torsion and bending of the cantilever. The sensitivity of this optical lever-detection system depends on the focal length f of the lens. The deflection of the laser light by the cantilever tilted by an angle α leads to lateral or vertical offset r of the position of the laser beam (on the quadrant photo-diode) during the measurement. Offset r is the measure for the bending or torsion of the cantilever. The second part of the measuring beam is used for the interferometrical measurement of the displacement (z) of the cantilever end with a measuring resolution of less than 0.1 nm. Moreover, a high-speed piezoelectric driver is added to increase the measuring dynamics and a shaker-piezo is added for non-contact measurement mode.

When doing the scan, the NPM machine operates the lateral scanning motion (along the X- and Y- axes) and makes it possible to use the entire NPM measuring range of 25 mm × 25 mm. The vertical motion and height adjustment of the specimen are performed with a combined movement of the high-speed piezoelectric drive of the probe and the NPM machine, respectively. The piezoelectric drive with its limited motion range (2 μ m) performs small, high-speed movements and the NPM machine is responsible for the large, low-speed movements, thus making the use of the entire measuring range of 5mm in Z-axis possible. All signals of the active probe are fed into the control unit of NPM machine for calibration and for calculating the profile information of the specimen.

For contact mode measurement, the bending of the cantilever (corresponding to the force between the tip and the surface of the sample) is controlled by a feedback loop. The feedback signal is the signal from the photo diode and serves as the input signal for the position control of the piezoelectric drive (Fig. 2).

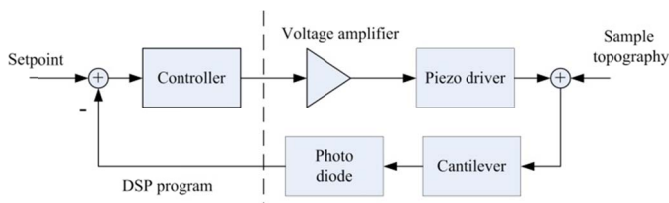


Fig. 2. Block diagram of the AFM control loop.

3. IDENTIFICATION OF THE PROBE DYNAMICS

In order to design the controller properly, a model of the probe's dynamics is obtained by black-box identification (Ljung, 1999). The input voltage of the amplifier (E-505, Physic Instrument) for piezoelectric drive (S-303, Physic Instrument) is regarded as the input of the active probe. The signal of the quadrant photodiode represents the output of the probe. A random noise generator running in a DSP (TI, TMS320C6713) is used to generate the excitation signal. The DSP then simultaneously records the input signal and the response of the active probe. These data then transfer to a personal computer for identifying the model. In the experiment, the sampling frequency is set to be 62.5K Hz.

The measured frequency response of the probe is shown in Fig. 3. After some trials, it is found that the response can be matched very well by a 20th order linear model. The discrete transfer function of the identified model is given by

$$G(z) = \frac{\sum_{j=1}^{20} b_j z^{-j}}{1 + \sum_{i=1}^{20} a_i z^{-i}}$$

Where the coefficients a_i and b_j are given in Table 1. For convenience, the frequency response of this model also shown in Fig. 3. Note that there are two obvious resonances at 1.15×10^5 and 1.39×10^4 rad/sec, and the order of the system model is high. The PI controller is not able to handle such kind of systems. If the H^∞ theory based controller is used, its order may as high as the model and makes it difficult to implement. In the next section, notch filters and PI controller are used to control this active probe.

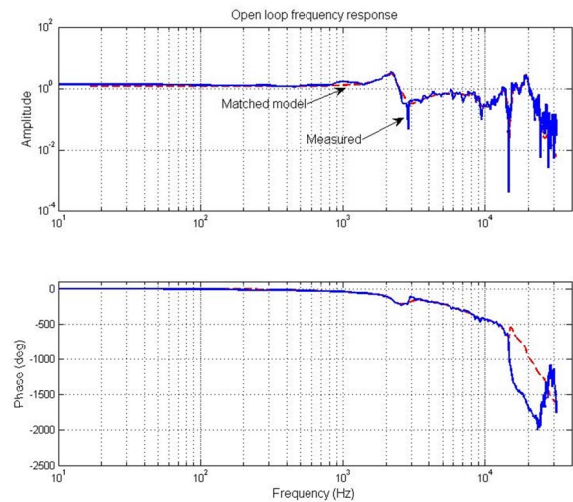


Fig. 3. Frequency responses of the active probe and the matched model.

4. CONTROLLER DESIGN

Generally, in commercial realization, PI controller is used to control the AFM. Therefore, a PI controller also designed for this active probe. For good robustness characteristics, we hope that the gain margin of the system near about 9dB and the phase margin near about 60°. After some trial, the PI controller was chosen as:

$$C_1(s) = 0.12\left(1 + \frac{4000}{s}\right)$$

This controller guarantees a gain margin of 8.59 dB and a phase margin of 94.2° and the corresponding bandwidth of the closed loop transfer function is about 84.6 Hz.

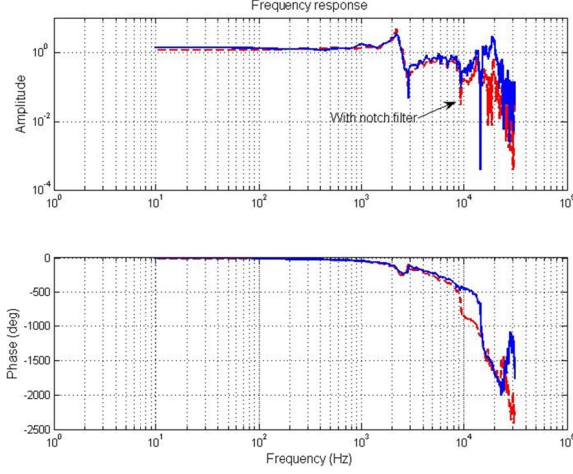


Fig. 4. The frequency response of the active probe with notch filter $N_1(s)$.

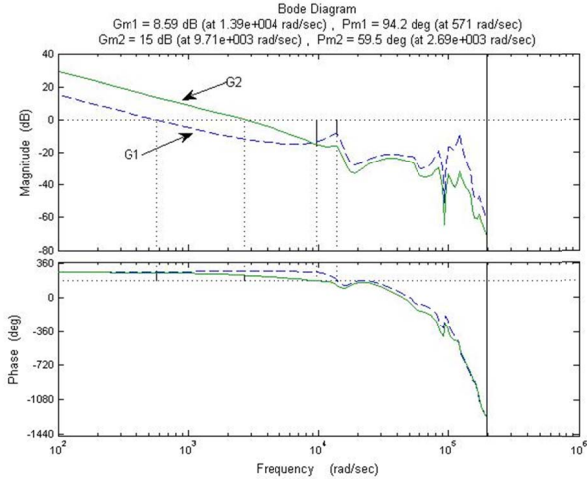


Fig. 5. Bode plots of the open-loop system without notch filters ($G_1(s) = C_1(s)G(s)$) and with the notch filters ($G_2(s) = C_1(s)N_1(s)N_2(s)G(s)$) where Gm1 and Gm2 are the gain margin, Pm1 and Pm2 are the phase margin of these two cases, respectively.

It is well known that the notch filter can be used to cancel out the sharp resonance peak in the frequency response and to improve the performance of PI controller (Abramovitch et al., 2009). In this study, the following two notch filters are added

$$N_i(s) = \frac{s^2 + 2\zeta_i\omega_i s + \omega_i^2}{s^2 + 2\omega_i s + \omega_i^2}$$

for $i=1, 2$, where $\omega_1 = 1.15 \times 10^5$, $\zeta_1 = 0.06$, $\omega_2 = 1.39 \times 10^4$, and $\zeta_2 = 0.25$. Fig. 4 shows the measured frequency response of the active probe with the notch filter $N_1(s)$. It can be seen that the resonance peak is removed. After removing the resonance peaks, the PI controller was retuned and was chosen as:

$$C_2(s) = 0.12\left(1 + \frac{20000}{s}\right)$$

With this PI controller and notch filters N_1 and N_2 , the gain margin and the phase margin of the system become 15dB and 59.2° respectively (Fig. 5), and the bandwidth of the closed loop system is 802.3 Hz. This is an enormous improvement over the PI controller.

5. EXPERIMENTAL RESULTS

The controllers that designed in last section were implemented in the DSP and some experiments were done to compare the performance of these two controllers.

In order to perform measurements correctly, the interferometrical active probe must be calibrated by the NPM machine and the characteristic line of the sensor must be determined. The electronics unit of the NPM machine then can use the coefficients of characteristic line to calculate the profile information of the specimen. The calibration can be accomplished in two steps.

The first step is the calibration of the bending signal of the optical lever-detection system with the piezoelectric drive disabled. In this test, the cantilever is brought to contact with a flat specimen surface. The specimen then moved up and down by the NPM machine at a range of 2 to 3 μ m. At the same time, the output signal of the active probe and NPM machine are sampled and saved simultaneously by the machine. Fig. 6 depicts the responses of this test. The working range and the operating point (i.e. the setpoint of the force that is needed for realising the constant-force measurement) are determined from this approach curve. By using this curve, the operation point is chosen to be 8200. The resolution of the characteristic line of the bending signal from the lever-detection system inside the working range is about 0.08 nm.

The second step is the calibration of the interferometer signal with the force control loop on (Fig. 7). The specimen is also moved up and down and the position of the cantilever is tracked simultaneously by the piezoelectric drive within its working range. In this case, the bending of the cantilever remains constant and equivalent to the setpoint. From the interferometer signal of the active probe shown in Fig. 7, it can be found that the hysteresis and creep of the piezoelectric drive have no influence on the measurement results and the working range of the force control is 2 μ m. Note that the calibration must be done again when the cantilever is replaced or re adjusted.

After calibrations were done, calibration grids with different height (100nm, 530nm, and 1000nm) were scanned with this metrological AFM at different scan speeds (10 μ m/s, 20 μ m/s, 50 μ m/s, and 100 μ m/s). Fig. 8 shows the standard deviation of the control error (cantilever bending) for scanning ten times. In all cases, the AFM that controlled by PI controller with notch filters (notch-PI) performs better. Note that the errors of scanning 1000nm height sample are much worse than that of scanning other samples. This is due to the limited working range (2 μ m) of the piezo driver.

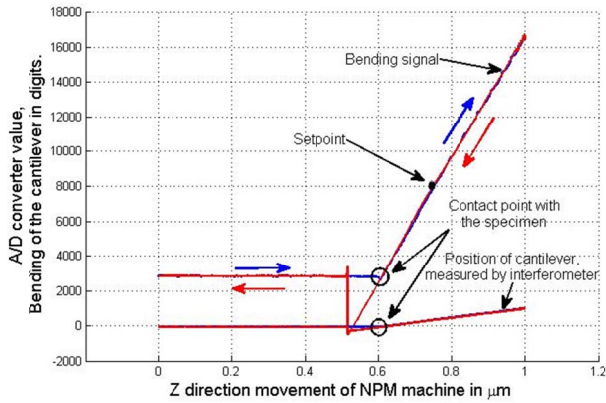


Fig. 6. Approaching curve of the AFM without force control.

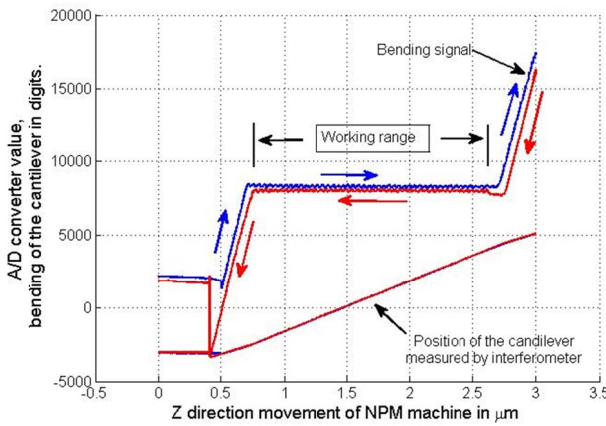


Fig. 7. Approaching curve of the AFM with force control.

Single line scan results of the calibration grid with 530nm height at different scan speeds are shown in Fig. 9 to compare the control performance of PI controlled AFM with notch-PI controlled AFM. The topography information of the specimen in the Y- direction is the position data of the NPM machine; profile height is the difference between the calibrated probe interferometer signal and the NPM machine's Z-axis position data. All of these data are determined by interferometer, the height of the sample is directly measurable and traceable to the standard of length. It can be found from Fig. 9 that the control error is smaller at all scan speeds in the case of the notch-PI controlled AFM comparing with the PI controlled one. Thus, the scan speed of the AFM can be increased by operating it with the notch-PI controller.

6. CONCLUSIONS

This paper has shown the design of a force controller for the active probe of a metrological AFM. For the design of the controller, the mathematical model of the active probe was identified. Notch filters were used to remove the major resonances of the system then the PI controller was retuned. Experimental results has shown that operating the AFM with this notch-PI controller can reduce the measurement error significantly and enables faster scanning compared with traditional PI controller. Moreover, the noticeable reduction of the cantilever deflection enables weaker scan forces preventing damage to tip and sample.

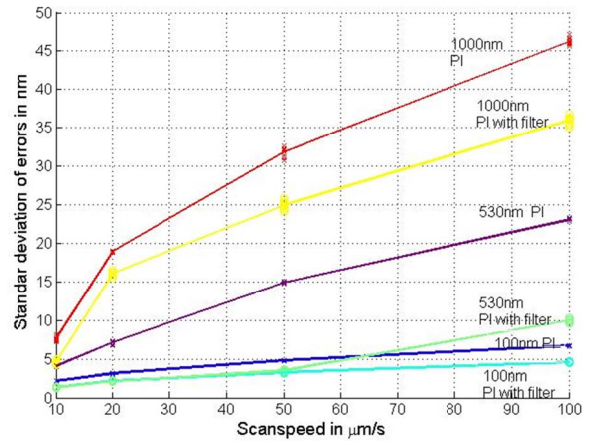


Fig. 8. The standard deviation of the control error signal (cantilever bending) of scanning different calibration grid at different scan speed with PI controlled and notch-PI controlled AFM.

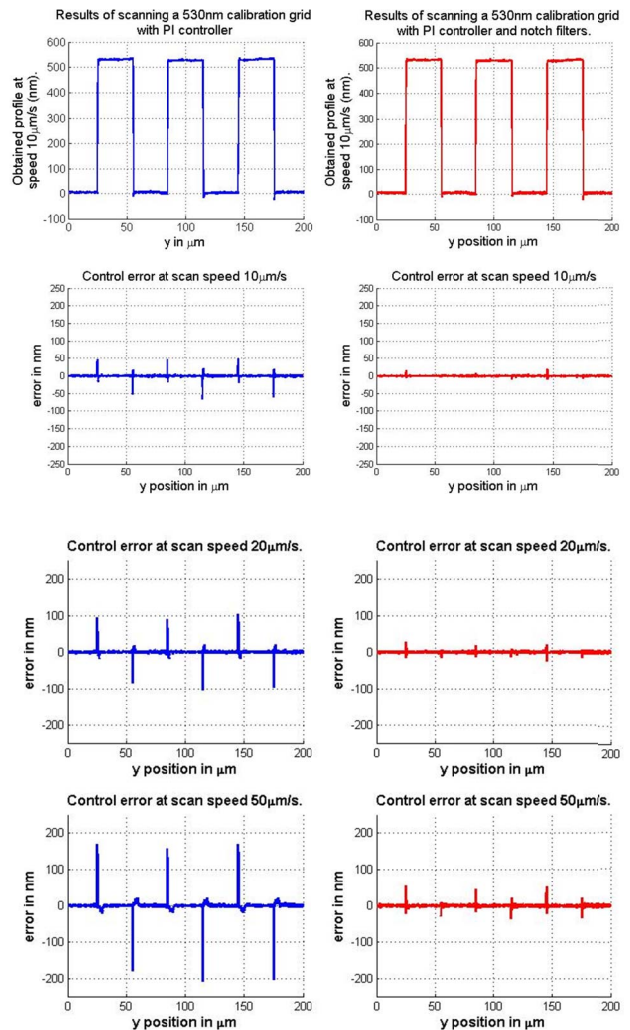


Fig. 9. Single line scan results of a 530nm height calibration grid with PI controlled AFM (left column) and the notch-PI controlled AFM (right column) at different scan speed.

REFERENCES

- Abramovitch, D.Y., Hoen, S., and Workman, R. (2009). Semi-Automatic Tuning of PID Gains for Atomic Force Microscopes. *Asian Journal of Control*, 11(2), 188-195.
- Binnig, G., Quate, C.F., and Gerber, C. (1986). Atomic force microscope. *Phys. Rev. Lett.*, 56(9), 930-933.
- Dorozhovets, N., Hausotte, T., Manske, E., Jager, G., and Hofmann, N. (2006a). Metrological scanning probe microscope. *Proc. SPIE* Vol. 6188, 155-162.
- Dorozhovets, N., Hausotte, T., Hofmann, N., Manske, E., and Jäger, G. (2006b). Development of the interferometrical scanning probe microscope. *Interferometry XIII: applications*. San Diego, Calif.
- Dorozhovets, N., Hausotte, T., Manske, E., and Jäger, G. (2008). Novel investigations and developments in a metrological scanning probe microscope. *Proceedings of ICPM*, 61-62, Ilmenau, German.
- Jaeger, G. (2010). Limitations of precision length measurements based on interferometers. *Measurement*, 43(5), 652-658.
- Ljung, L. (1999). *System Identification: Theory for the User*. 2nd ed., Prentice Hall, Upper Saddle River, New Jersey.
- Merry, R., Uyanik, M., Molengraft, R., Koops, R., Veghel, M., and Steinbuch, M. (2009). Identification, Control and Hysteresis Compensation of a 3 DOF Metrological AFM. *Asian Journal of Control*, 11(2), 130-143.
- Sarid, D. (1994). *Scanning Force Microscopy*. Oxford University Press, New York.
- Schitter, G., Stemmer, A., and Allgower, F. (2004). Robust Two-Degree-of-Freedom Control of an Atomic Force Microscope. *Asian Journal of Control*, 6(2), 156-163.
- Zou, Q., Leang, K.K., Sadoun, E., Reed, M.J., and Devasia, S. (2004). Control Issues in High-Speed AFM for Biological Applications: Collagen Imaging Example. *Asian Journal of Control*, 6(2), 164-178.

ACKNOWLEDGEMENT

The first author would like to thank the financial support of the National Science Council of Taiwan (99-2918-I-150-002, 98-2221-E-150-037-MY2), Professor Gerd Jäger and to greatly acknowledge the assistance of Henner Baitinger.

Table 1. Coefficients of the model.

i	1	2	3	4	5	6	7	8	9	10
a_i	-0.1411	0.3293	-0.6104	-0.1141	-0.1603	0.0819	0.0646	-0.0562	-0.0197	0.1019
b_i	-0.0091	-0.0121	-0.0084	0.0036	0.0162	0.0457	0.2543	0.3739	0.0933	-0.0894
i	11	12	13	14	15	16	17	18	19	20
a_i	0.2779	0.2152	0.0430	-0.1138	0.0028	-0.1647	0.2561	0.0107	0.0425	-0.1272
b_i	0.0284	-0.0910	-0.1084	0.1023	0.0448	-0.0484	0.1377	0.2473	0.0955	0.0043